

Comparison of Nanosized Gold-Based and Copper-Based Catalysts for the Low-Temperature Water–Gas Shift Reaction

Diogo Mendes,[†] Hermenegildo Garcia,[‡] V. B. Silva,[†] Adélio Mendes,[†] and Luis M. Madeira^{*,†}

LEPAE, Chemical Engineering Department, Faculty of Engineering, University of Porto, Rua Dr. Roberto Frias, 4200-465 Porto, Portugal, and Instituto de Tecnología Química, UPV-CSIC, Universidad Politécnica de València, Av. de los Naranjos s/n, 46022 Valencia, Spain

In this paper the catalytic performances for the low-temperature water–gas shift reaction of Au/TiO₂ type A (from World Gold Council), Au/CeO₂ (developed at UPV-CSIC), CuO/Al₂O₃ (from BASF), and CuO/ZnO/Al₂O₃ (from REB Research & Consulting) have been compared. The catalysts were characterized by different techniques such as Raman spectroscopy, BET surface area measurements, temperature-programmed reduction, and high-resolution transmission electron microscopy, which gave additional information on the redox properties and textural and morphological structure of the investigated samples. The performances of these catalysts were evaluated in a wide range of operating conditions in a micro packed-bed reactor. It was observed that the presence of reaction products in the feed (CO₂ and H₂), as well as CO and H₂O feed concentrations, have significant effects on the catalytic performances. With a typical reformat feed the Au/CeO₂ catalyst reveals the highest CO conversion at the lowest temperature investigated (150 °C). However, while in the long tests performed the CuO/ZnO/Al₂O₃ catalyst showed a good stability for the entire range of temperatures tested (150–300 °C), the Au/CeO₂ sample clearly showed two distinct behaviors: a progressive deactivation at lower temperatures and a good stability at higher ones. The selection of the best catalytic system is therefore clearly dependent upon the range of temperatures used.

1. Introduction

Anthropogenic carbon dioxide (greenhouse gas) is the most responsible pollutant for increased global warming. It is released into the atmosphere mainly through burning of fossil fuels (e.g., coal, petrol, and diesel), and these emissions are expected to increase following the growth in world population and economy in the coming years.¹ One of the most important developments, as a clean-alternative energy source for the future, is proton-exchange membrane fuel cells (PEMFCs) that operate using hydrogen at low temperatures. In situ fuel processing is a very promising method of supplying hydrogen to PEMFCs due to the difficulties associated with long-distance transportation and hydrogen storage.² In a typical operation, however, gas emerges from the reformer with a CO level of 1–10 vol %, which adsorbs irreversibly on the Pt catalyst of the PEMFC anode, decreasing the fuel cell performance. Therefore, fuel processors must be designed to convert the CO content in the fuel stream to levels that are tolerated by Pt (less than 100 ppmv).³ In this sense, the water–gas shift (WGS) reaction ($\text{CO} + \text{H}_2\text{O} \leftrightarrow \text{CO}_2 + \text{H}_2$) has been considered and extensively studied. Besides, it simultaneously favors H₂ fuel stream enrichment that may be followed by a final purification step, which may involve preferential oxidation or methanation of residual CO.^{4,5} Because the WGS is an exothermic reaction ($\Delta H_{298\text{K}} = -41.1 \text{ kJ mol}^{-1}$), high conversions can only be achieved at low temperatures. On the other hand, under such conditions the reaction is controlled by the kinetics, so highly active and stable low-temperature WGS catalysts are needed.

From the point of view of “on-board” fuel processor applications, these catalysts must obey other requirements, such as nonpyrophoricity and stability toward condensation and poisons

such as chlorine and sulfur, and additionally should require no exceptional pretreatments.^{4,5} Until recently, the shift reactors in fuel cell systems at the kilowatt scale have utilized industrial iron- and copper-based catalysts. Fe–Cr formulations have the advantages of being cheap, stable, and able to withstand gas-phase impurities such as S and Cl compounds. However, they need temperatures above 350 °C to be active.⁶ The Cu-based formulations have good activity even below 200 °C, but are susceptible to poison and operate in a limited temperature range due to the Cu sintering that occurs above 300 °C.⁷ Other disadvantages of Cu materials are the need of activation, before operation, by a slow and controlled reduction process. Besides, upon shutdown the catalyst must be purged with an inert gas to prevent condensation and reoxidation; otherwise its performance becomes significantly impaired. Repeated start-up/shutdown cycles, as associated with in-vehicle use, may well result in condensation of water and subsequent deactivation of the catalyst. Extensive research has therefore been conducted looking for better solutions to these well-known commercial WGS catalysts. In fact, the CuO/ZnO/Al₂O₃ formulation seems to be the reference standard for the development of other WGS catalysts.

Reducible oxide-supported nanosized gold and platinum catalysts seem to be promising candidates for on-board fuel processing, mainly due to their high activity at low temperatures and potential stability in an oxidizing atmosphere.^{8–10} Selection between both catalysts is however delicate because most available data are presented for very specific experimental conditions, not only in what concerns the preparation and pretreatments of the catalysts, but also regarding the operating conditions used in activity tests. Burch¹¹ pointed out that a well-prepared, carefully activated gold catalyst can be at least as active as an equivalent platinum catalyst, and if the best available samples are considered, then gold is apparently significantly more active than platinum. Even though gold catalysts have the advantage to possess greater thermal stability than CuO/ZnO

* To whom correspondence should be addressed. Tel: +351 22 508 1519. Fax: +351 22 508 1449. E-mail: mmadeira@fe.up.pt.

[†] University of Porto.

[‡] Universidad Politécnica de València.

formulations, their activity is very sensitive to the preparative procedure, the gold particle size, and the intimate metal–support contact.^{11–13}

High catalytic activity for the WGS reaction using gold-based catalysts operating at low temperature was reported for the first time using nanosized Au/ α -Fe₂O₃.¹⁴ In 1997, Sakurai et al.¹² used Au/TiO₂ for both forward and reverse WGS reactions presenting high activities. Since that time, many studies have revealed that highly dispersed gold on different metal oxide supports, e.g., ZrO₂,^{15,16} CeO₂,^{13,17–19} and Al₂O₃,¹⁴ is catalytically active for the WGS reaction at low temperatures. However, the combination of Au with nanosized ceria has apparently been shown to be the most active low-temperature WGS gold catalyst.^{11,20}

Due to the lack of a systematic study in which the most promising catalytic systems are tested under similar conditions, in this work the catalytic performances of various commercially available catalysts, namely, Au/TiO₂ type A (World Gold Council), CuO/Al₂O₃ (BASF), CuO/ZnO/Al₂O₃ (REB Research & Consulting), and a laboratory-made one, Au/CeO₂, for conducting the WGS reaction at temperatures ranging from 150 to 300 °C are compared. The experimental tests were carried out in a micro fixed-bed reactor where criteria parameters such as the CO conversion level and stability were used to perform catalyst evaluation and selection. The runs were done in a wide range of operating conditions (steam/gas ratio and temperature) under a typical reforming feed composition. Several characterization techniques have also been employed to provide insight into the properties of the investigated samples.

2. Experimental Section

2.1. Catalyst Preparation. The gold–ceria sample was prepared by the deposition–precipitation method. First, nanoparticulated ceria was prepared by adding, under stirring, at ambient temperature, an ammonia aqueous solution (1.12 L, 0.8 M) over 375 mL of Ce(NO₃)₄ (0.8 M). The colloidal dispersion of CeO₂ nanoparticles was heated in a poly(ethylene terephthalate) (PET) vessel at 100 °C for 24 h. The resulting yellow precipitate was filtered and dried under vacuum overnight. The cerium oxide synthesized, which was prepared following a procedure previously described,²¹ has a very high surface area (180 m²·g⁻¹), owing to the small size of the nanoparticles (~5 nm). Then Au was deposited on the nanoparticulated ceria using the following procedure: a solution of HAuCl₄·3H₂O (270 mg) in 160 mL of deionized water was brought to pH 10 by addition of a 0.2 M NaOH solution. Once the pH value was stable, the solution was added to a gel containing colloidal CeO₂ (4.01 g) in H₂O (50 mL). After adjustment of the pH of the slurry to a value of 10 by adding a 0.2 M solution of NaOH, the slurry was maintained at room temperature under vigorous stirring for 18 h. The Au/npCeO₂ solid was then filtered and exhaustively washed with several liters of distilled water until no traces of chlorides were detected by the AgNO₃ test. The catalyst was dried under vacuum at room temperature for 1 h. Then 3.5 g of the supported catalyst was added over 30 g of 1-phenylethanol at 160 °C, and the mixture was allowed to react for 20 min (this ensures complete reduction of gold nanoparticles). The catalyst was filtered, washed with acetone and water, and dried under vacuum at room temperature. The total Au content of the final Au/npCeO₂ catalyst was 1.5 wt %, as determined by chemical analysis. This catalyst (Au/npCeO₂) is commercially available from ITQ (Web page www.upv.es/itq).

The Au/TiO₂ catalyst was bought from the World Gold Council (U.K.) and is referred to as a reference Au catalyst (type A). The CuO/Al₂O₃ sample (CU-1271, Selectra Shift) was supplied by BASF (Germany), and the CuO/ZnO/Al₂O₃ commercial catalyst (~50 wt % CuO and 40 wt % ZnO) was acquired from REB Research and Consulting, Ferndale, MI. Both Cu-based catalysts were crushed and sieved to give a particle size of <180 μm (similar to that of the powdered gold solids).

2.2. Catalyst Characterization. The BET surface area of the samples was analyzed by nitrogen adsorption at 77 K with a Micromeritics 2000 ASAP automated gas sorption analyzer. The samples were exhaustively outgassed at 450 °C under vacuum before area measurements.

For crystal analysis and indexation, Au/npCeO₂ samples were examined by bright- and dark-field electron microscopy with a Jeol 2200 HRTEM instrument operated at an accelerating voltage of 200 kV. Chemical analyses of gold in the catalysts were carried out after the solids were dissolved by attack with a 2:1 mixture of HNO₃/HF on a Varian-10 Plus atomic absorption spectrometer or directly on the solids using a Philips Minipal 25 fm analytic X-ray apparatus and a calibration plot.

Raman spectra were recorded at room temperature and ambient atmosphere using a Renishaw inVia microscope with a diode laser (785 nm) and averaging 10 scans of different areas of the black solid.

Finally, temperature-programmed reduction (TPR) measurements were performed in a Micromeritics Autochem 2910 equipped with a TCD detector. The mixture of 10% H₂ in He as the reducing gas was used in all experiments, and a temperature ramp of 5 °C·min⁻¹ was employed.

2.3. Experimental Reaction Apparatus, Procedures, and Analysis. The catalytic activity determined for the WGS reaction is expressed as the degree of CO conversion. The experiments were carried out using a micro packed-bed reactor operating isothermally and at atmospheric pressure, as can be seen in Figure 1. The 6 mm i.d. stainless steel reactor was encased in an electric oven (Mettler, type UNE200), controlled by a programmable temperature controller. The reactor was typically loaded with 250 mg of the catalyst, supported by two fritted Teflon disks to avoid the catalyst powder dispersion over the pipes. In the stability tests, the reactor was loaded with 150 mg of catalyst. A thermocouple was introduced from the top of the reactor, and it was placed at the center of the catalyst bed, which was shown to operate under isothermal conditions (within ±2 °C).

All the WGS catalysts were activated in situ with a mixed gas flow of H₂/N₂ measured by means of mass flow controllers. The reduction protocols applied were based on literature information to ensure complete metal oxide reduction, without sintering.^{22,23} For Cu-based catalysts the prerduction protocol considers heating the catalyst, in nitrogen, from room temperature to 80 °C; then the reduction mixture (5 vol % H₂/N₂, total flow rate of 30 mL_N min⁻¹) is admitted, and the samples are heated at 5 °C·min⁻¹ from 80 to 230 °C and maintained at this temperature for 4 h. Nevertheless, the terminology used when referring to these samples is the commercial one, which makes reference to the copper oxide state. For Au-based catalysts the prerduction protocol considers heating to 200 °C in a N₂ stream and keeping the solids at this temperature for 30 min. Subsequently, reduction is performed for 45 min in a 10 vol % H₂/N₂ stream (at a total flow rate of 30 mL_N min⁻¹), followed by 30 min in a N₂ flow, both at 200 °C. In all cases, after reduction, the catalysts were cooled or heated to the reaction temperature

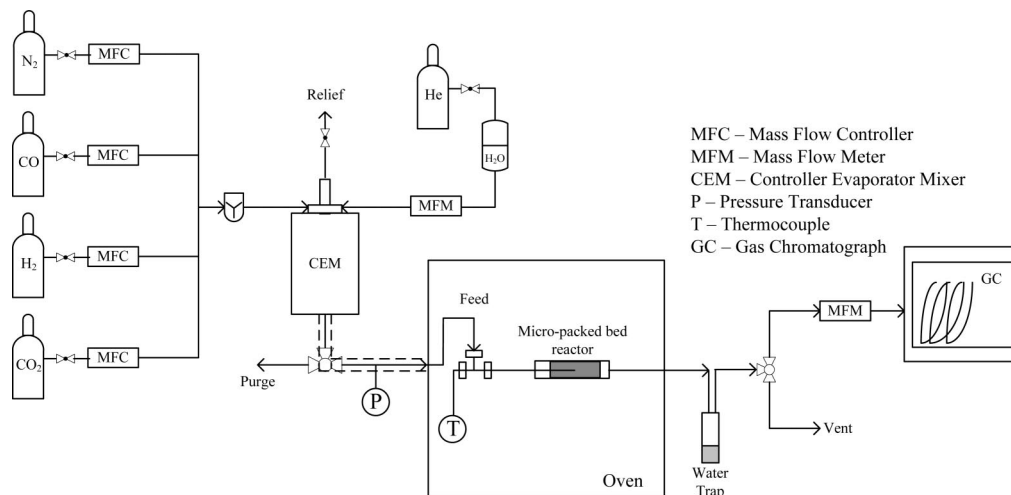


Figure 1. Sketch of the experimental setup.

and the reactor was flushed with N_2 prior to the introduction of the reaction mixture. To avoid overheating of the catalyst bed and subsequent metal particle sintering, strict temperature and hydrogen flow rate controls were performed.

The reaction was started by introducing, for instance, a typical reforming gas mixture of 4.70% CO, 34.78% H_2O , 28.70% H_2 , 10.16% CO_2 , and 21.66% N_2 (vol %) in the reactor feed, using four mass flow controllers (cf. Figure 1). Deionized water was metered, vaporized, and mixed in a controller evaporator mixer (CEM; Bronkorst) system with the other gases before entering the reactor. The GHSV (gas hourly space velocity) was fixed at $4800 \text{ mL}_N \cdot \text{g}_{\text{cat}}^{-1} \cdot \text{h}^{-1}$ and the reaction temperature varied between 150 and 300 °C. The reactor outlet stream was passed through a condenser to remove water for further analysis. The gas-phase products were then analyzed in an online gas chromatograph (Dani 1000 GC). A chromatographic column (Supelco Carboxen 1010 plot, from Sigma-Aldrich, 30 m \times 0.32 mm i.d.), with He as the carrier gas ($1 \text{ mL}_N \text{ min}^{-1}$) and a TCD (Valco thermal conductivity detector), was used to analyze N_2 , CO, and CO_2 . The carbon and the nitrogen molar balance relative errors were typically lower than 10%. Regarding hydrogen, it is well-known that it is difficult to measure its composition by GC with the used detector since its thermal conductivity is close to that of helium, the carrier gas. Therefore, the H_2 composition in the gas streams was calculated from the mass balance (difference from 100%, dry basis), which is required for mass flow rate corrections. During the analysis, a temperature program was used as follows: (i) isothermal operation at 35 °C for 7.5 min; (ii) heating from 35 to 80 °C with a rate of $10 \text{ }^\circ\text{C} \cdot \text{min}^{-1}$; (iii) keeping the sample at 80 °C for 8 min. All the pipes and valves along the water feed stream and in the reactor exit were heated to 130 °C to prevent the condensation of water.

3. Results and Discussion

3.1. Characterization of the Samples. The structural and morphological properties of the samples used in this work were first investigated. The metal loading (in the case of copper samples, this refers to the oxide form), the surface areas of the formulations, and the average size of the metal particles, as estimated by the HRTEM technique, are given in Table 1.

As illustrated in Figure 2, spherical copper particles homogeneously distributed on the respective surface were obtained for the $\text{CuO}/\text{Al}_2\text{O}_3$ sample, for which HRTEM results indicate an average size of around 9.2 nm (cf. Table 1). The low copper

Table 1. Physical Properties of the Studied Samples

sample	active metal loading (wt %)	S_{BET} (m^2/g)	av metal particle size (nm)
$\text{CuO}/\text{Al}_2\text{O}_3$	5–20 ^a	110	9.2
$\text{CuO}/\text{ZnO}/\text{Al}_2\text{O}_3$	~50 ^a	9.0	6.9
Au/TiO_2	1.5 ^a	37	4.0
Au/CeO_2	1.5	180	4.4 ^b

^a Data given by the manufacturer. ^b A total of 200 particles were counted, due to the poor contrast between gold and ceria.

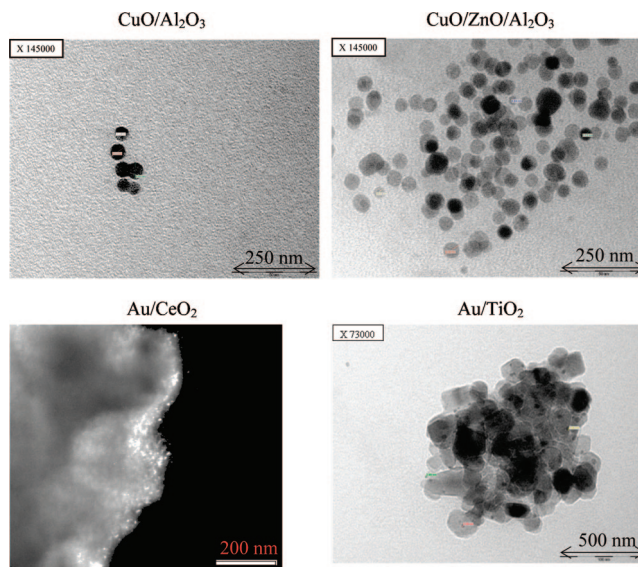


Figure 2. TEM pictures of the catalyst samples studied.

content in this catalyst is evident in the picture since only a little aggregation is seen. For the $\text{CuO}/\text{ZnO}/\text{Al}_2\text{O}_3$ solid the smaller particle size and the higher copper loading are perceptively presented in the picture since a higher density of CuO particles (aggregation) is seen (Figure 2). This also occurs for the Au-based catalysts, in which the particle size is even smaller, being particularly noticed for the Au/TiO_2 sample. HRTEM was used to report the size of gold nanoparticles. Therefore, the gold nanoparticles have been identified by the fringe distance shown in Figure 3 that corresponds to the gold interatomic distance.

The catalysts were also studied by Raman spectroscopy (Figure 4). In the case of $\text{CuO}/\text{Al}_2\text{O}_3$ no peaks were recorded, probably due to the strong fluorescence of the material. In contrast, for $\text{CuO}/\text{ZnO}/\text{Al}_2\text{O}_3$ and Au/CeO_2 the peaks charac-

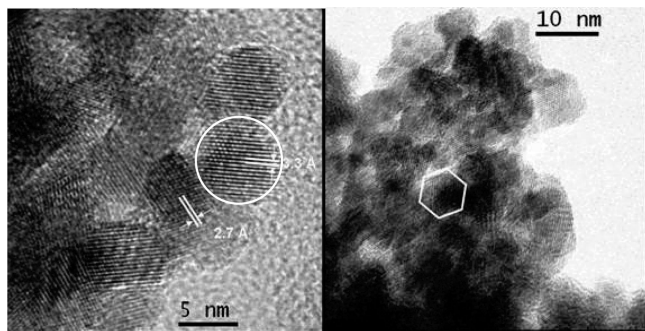


Figure 3. HRTEM picture of the Au/CeO₂ catalyst.

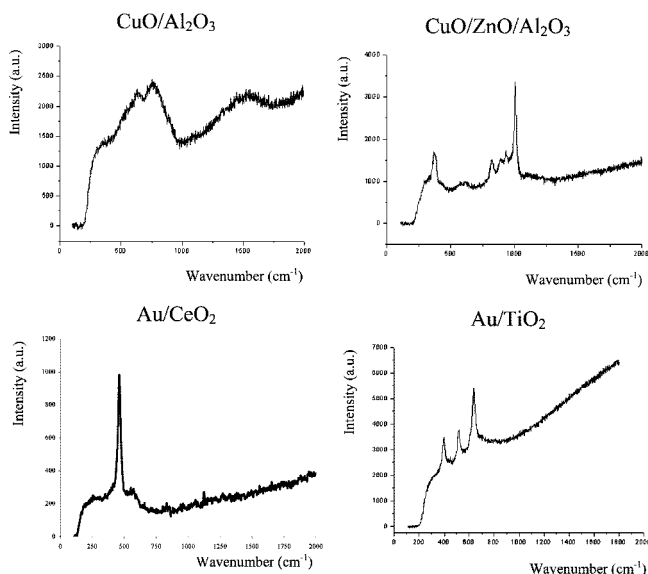


Figure 4. Raman spectra of the catalysts studied in this work.

teristic of ZnO (380 cm⁻¹) and CeO₂ (475 cm⁻¹) were observed. In the latter sample, the observed peak corresponds to the Ce–O vibration bond. The Au–Au vibration appears below 200 cm⁻¹ and is not visible due to the low loading of the materials and the low intensity of the peak. From the Au/TiO₂ Raman spectrum it can also be concluded that titanium dioxide is predominantly constituted by the anatase phase (due to the well-known TiO₂ anatase bands at 398, 516, and 640 cm⁻¹).

The TPR technique was used to evaluate the reducibility of the synthesized sample, before and after Au addition to the ceria support. The redox characteristics of this type of catalyst are known to be relevant for their performance in the WGS reaction. Comparison of the TPR profiles of CeO₂ and Au/CeO₂ clearly reveals that the presence of gold nanoparticles on the surface of the ceria support exerts a remarkable influence, favoring the reducibility of this metal oxide (Figure 5). Thus, the reduction peak that appears at about 470 °C in CeO₂ becomes considerably shifted to much lower temperatures (about 95 °C) when gold nanoparticles are present in the solid. The peak in the TPR profile at 63 °C is most probably related to the reduction of oxygen species, adsorbed during calcination in air, on some nanogold particles smaller than 2 nm, in accordance with Boccuzzi et al.²⁴ In conclusion, Figure 5 shows the reducibility increase of the Au/CeO₂ sample with the TPR promotional effect of gold on the surface reduction of ceria, leading to the creation of oxygen vacancies. Therefore, the gold particles located in close contact with these oxygen-vacancy defects of ceria may be very active sites for WGS reaction.

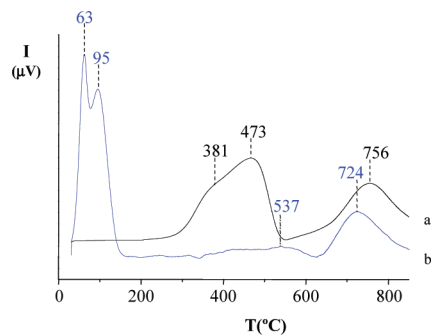


Figure 5. Temperature-programmed reduction by hydrogen of CeO₂ (a) and Au/CeO₂ (b).

3.2. Catalytic Tests. In this section the catalytic performance of Au/CeO₂ toward the WGS reaction is compared with that of three commercial catalysts: (i) Au/TiO₂, purchased from the World Gold Council and which has the same Au content and a similar average particle size (cf. Table 1); (ii) the commercial CuO/Al₂O₃ (CU-1271, Selectra shift) received from BASF; (iii) the commercial CuO/ZnO/Al₂O₃ purchased from REB Research & Consulting. The catalytic tests started by performing experiments using two different feeds: one with just CO and H₂O (diluted in He) and the other with a typical reformat composition (4.70% CO + 34.78% H₂O + 28.70% H₂ + 10.16% CO₂ + 21.66% N₂). The effects of H₂O and CO concentration in the feed are also important to analyze, and this was therefore done for each catalyst, at different temperatures. Data presented below concern the steady state (each data point in the graphs results from the average of at least three analyses; the maximum standard deviation obtained was 1.5%) with the exception of the Au/CeO₂ sample, because in this case some catalyst deactivation was observed (see section 3.2.4 regarding stability tests). For this reason the activity measurements for this sample began at high temperatures (in which deactivation is negligible) and ended at low temperatures, the CO conversion being measured in the first 10 000 s until a relative error below ca. 5% was obtained, in three consecutive analyses. During the night, the catalysts being tested were under a N₂ atmosphere to avoid reoxidation.

3.2.1. Effect of Reaction Products in the Feed Composition. Figure 6 illustrates the effect of the reaction products (H₂ and CO₂) on the performance attained by each catalytic system at different temperatures. As expected, the CO conversion increases with the reaction temperature due to the kinetic constraints, in some cases approaching the thermodynamic equilibrium conversion (dashed lines in the figures). After this point, the conversion decreases due to the exothermic nature of the reaction. The equilibrium conversion ($X_{\text{CO,eq}}$) values were calculated on the basis of the equilibrium constant ($K_p = \exp[(4577.8/T) - 4.33]$, where T is in kelvin) obtained by Moe.²⁵ Assuming ideal gas behavior, the equilibrium conversion was then obtained by solving the following equation, where K_p is expressed on the basis of the feed composition ($y_{i,\text{in}}$ refers to the molar fraction of species i at the reactor inlet):

$$K_p = \frac{(y_{\text{CO}_2,\text{in}} + y_{\text{CO,eq}}X_{\text{CO,eq}})(y_{\text{H}_2,\text{in}} + y_{\text{CO,eq}}X_{\text{CO,eq}})}{(y_{\text{CO,eq}}(1 - X_{\text{CO,eq}}))(y_{\text{H}_2\text{O,eq}} - y_{\text{CO,eq}}X_{\text{CO,eq}})} \quad (1)$$

Under only CO and water in helium, catalysts CuO/Al₂O₃, CuO/ZnO/Al₂O₃, and Au/CeO₂ reveal a similar CO conversion that is higher than that reached by the Au/TiO₂ sample in the entire range of temperature tested (Figure 6). At 150 °C and for the first group of catalysts, the CO conversion reached is

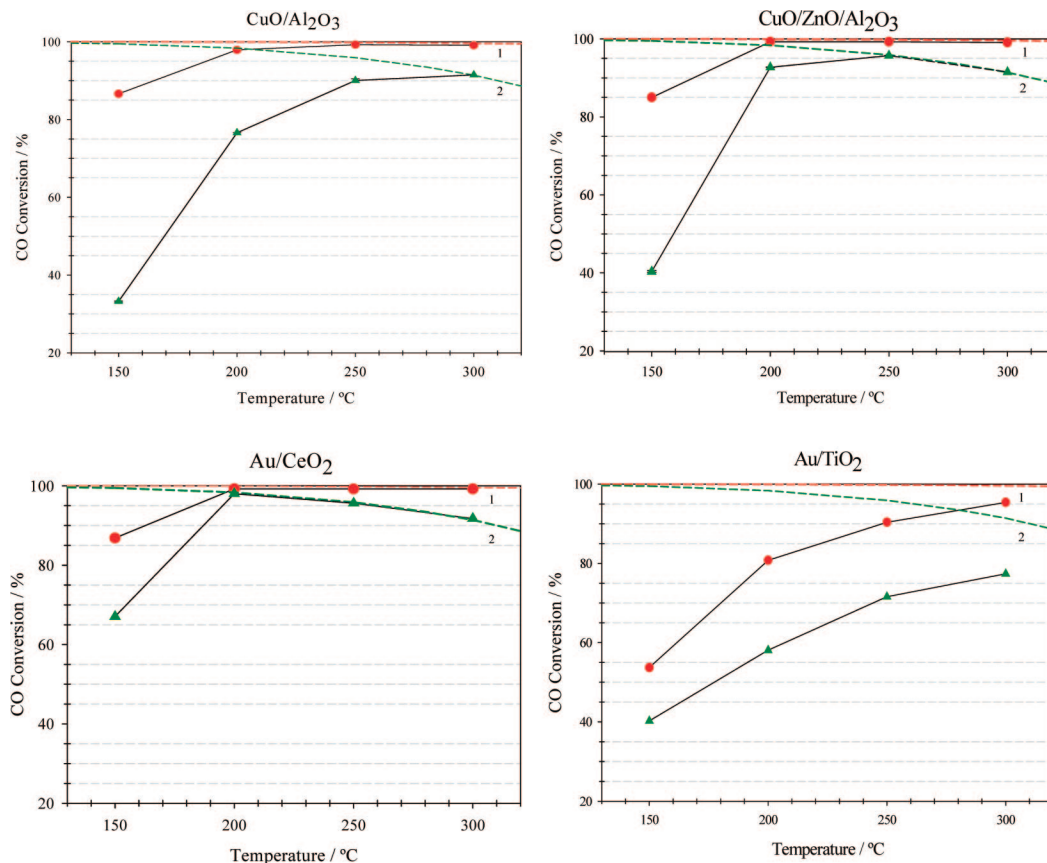


Figure 6. Effect of reaction products in the feed stream over the CO conversion for each catalyst at different temperatures. The lines represent the thermodynamic conversion. Feed composition: (●, 1) 4.74% CO + 35.39% H₂O + 59.87% He, (▲, 2) 4.74% CO + 35.39% H₂O + 28.46% H₂ + 10.06% CO₂ + 21.35% N₂.

similar and approximately 86%, although for the Au/CeO₂ formulation this value is already affected by some deactivation noticed at low temperatures (cf. section 3.2.4 about stability tests). At higher temperatures the CO conversions tend to that predicted by the thermodynamics, but are always higher than that exhibited by the Au/TiO₂ catalyst.

The detrimental effect of H₂ and CO₂ in the feed stream is clearly noted in all the catalysts tested, in agreement with Le Chatelier's principle (reaction equilibrium shifts in the opposite direction, toward reactant formation, decreasing CO conversion). Several authors use empirical power law models to fit the kinetic data. Most of them show the negative effect of the presence of one or both reaction products.^{26–28} In our case, the major difference was obtained for the CuO/Al₂O₃ sample at 150 °C, reaching a CO conversion of only 33% when the reaction products are present in the reactor feed, compared with 87% in their absence. At 150 °C both Cu-based catalysts are shown to be strongly affected by the presence of CO₂ and H₂. However, this drawback seems to be attenuated with the temperature increase. The presence of ZnO seems to be important in terms of the performance reached, i.e., in terms of tolerance to the presence of hydrogen and carbon dioxide. It is worth noting that the role of ZnO and Al₂O₃ regarding the WGS activity and the nature of the active sites for copper-based catalysts is still controversial. Besides their role as structural promoters,^{29–32} both oxides gathered some literature support working also as chemical promoters. In fact, several authors observed an enhancement in the catalytic activity of Cu supported on ZnO due to synergetic effects responsible for improved covalency between the different oxidation states of copper in the metal lattice.^{22,33–35} Moreover, the catalytic performance improvement

from binary CuO/ZnO to ternary CuO/ZnO/Al₂O₃ catalysts reveals the effect of adding alumina; alumina is reported to form a hydroxalite phase that improves the catalyst performance.²² On the other hand, the lower copper loading in the CuO/Al₂O₃ catalyst (see Table 1) might influence the lower CO conversion obtained with this sample.

Under the operating conditions of Figure 6, the Au/CeO₂ sample shows the best performance. It is known that, for Au-based catalysts, the synthesis method (which was the same for both samples—deposition/precipitation) and corresponding conditions affect their WGS performance. Nevertheless, the influence of the gold support (ceria or titania) may have a major role in terms of their activity. As succeeds with Cu-based catalysts, many authors believe that the WGS reaction on supported noble materials, namely, on reducible metal oxides (CeO₂, TiO₂, ZrO₂,...), is a bifunctional system too. The reaction mechanism is assumed to be conducted in two different sites: the dispersed metallic phase, which is mainly responsible for adsorption/activation of CO, and the metal oxide support, which is hydrophilic in nature and is mainly responsible for adsorption/activation of H₂O.^{36–38} Both ceria and titania have the capacity to be reduced under the WGS reaction conditions. Several authors refer to the reducibility of the support as being an important key to a higher catalyst activity due to the formation of either oxygen vacancies within the support or partially reduced sites at the metal–support interface.^{17,37–40} Thus, the higher WGS activity obtained with the ceria-supported catalyst can be due to its higher redox capacity and mobility of the surface oxygen/hydroxyl group when compared with the titania-supported catalyst. Indeed, Idakiev et al.⁴¹ also found a shift of the TPR peak to low temperatures after incorporation of Au in

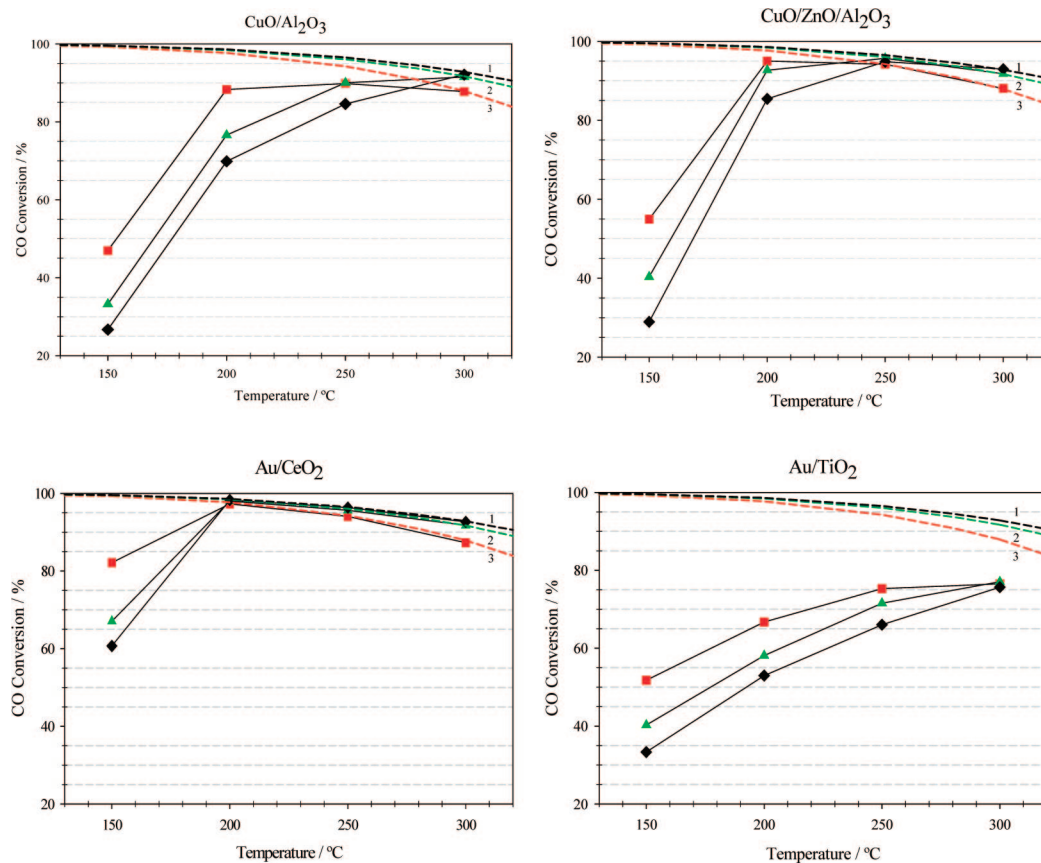


Figure 7. Effect of the CO content in the feed stream composition over the CO conversion for each catalyst at different temperatures. The lines represent the thermodynamic conversion. Feed composition: (◆, 1) 9.42% CO, (▲, 2) 4.74% CO, (■, 3) 2.38% CO. In all cases the rest of the feed is 35.39% H₂O, 28.46% H₂, 10.06% CO₂, and the balance N₂.

TiO₂ (from 400 to 100 °C), but the intensity of such a low-temperature peak is almost negligible compared to that of the original support, in opposition to what happens for the Au/CeO₂ sample (see section 3.1). Finally, the higher surface area of the ceria support, also responsible for a better metal dispersion, is certainly an important parameter for the activity enhancement attained.

3.2.2. Effect of the CO Content in the Feed. The effect of the CO content in the feed stream is also important to analyze due to the inherent implications on the thermodynamic equilibrium. In addition, this also allows to study the performance of WGS catalysts under different feed compositions as happens when the WGS feed proceeds from different steam-reforming processes and hydrocarbon feedstocks. The effect of the CO concentration on the conversion is illustrated in Figure 7.

The CO concentration decrease in the gas feed produces an increase in the performance of all catalysts, at least at 150 °C. This behavior seems to be not consistent with that predicted by Le Chatelier's principle, but is also observed in other works.^{19,27} Amadeo and Laborde²⁷ studied the influence of the partial pressure of the WGS reactants and products on the CO conversion over a copper-based commercial catalyst at 503 K. The authors justified the observed negative effect by the proportional formation of CO₂ when the feed CO partial pressure increases. In the work by Luengnaruemitchai et al.,¹⁹ the effect of CO and H₂O concentrations over the catalytic performance of Au/CeO₂ was studied, with an idealized feed consisting of 0.5–2% CO and 2.6% H₂O in helium. However, no explanation was given for the negative effect of the increasing CO concentration for this catalytic system. Nevertheless, as the temperature increases the catalytic systems tested in this work

tend to create a “zone” where the effect of the CO concentration on the catalytic performance is less significant, revealing that its effect on the conversion can change with the reaction temperature (Figure 7). However, this zone is located at different temperatures, according to the higher or lower catalyst activity. Beyond that region, the data tend to follow the equilibrium conversion lines, as predicted by Le Chatelier's principle (the conversion is higher for higher CO contents in the reactant feed, because this shifts the equilibrium).

For Cu-based WGS catalysts different reaction orders regarding CO concentration have been reported. For instance, Ayastuy et al.²⁶ and Ovesen et al.²⁸ reported a unity order of reaction with respect to CO over ternary Cu-based catalysts. On the other hand, Salmi and Hakkarainen⁴² reported variable CO reaction orders as a function of temperature, ranging from 1 to 0.45. For Au/CeO₂ catalysts Leppelt et al.²³ reported a CO reaction order of 0.5. In fact, for all WGS catalysts studied the CO positive reaction order is verified only above a certain temperature. The negative (retardation) effect observed in this work for both Cu and Au catalysts at lower temperatures can be explained on the basis of the associative mechanism, namely, on the intermediate species (formates and/or carbonates) formed during the reaction. Once the CO concentration increases, the formation of intermediate species also increases. At lower temperatures, the coverage of this species over the catalyst surface increases for both copper-based⁴³ and gold-based⁴⁴ catalysts due to a slower decomposition of these intermediates into the final reaction products. Therefore, a blocking effect of the active sites by the reaction intermediates, which is more severe at lower temperatures, should happen, decreasing the overall CO conversion; this is also behind the deactivation

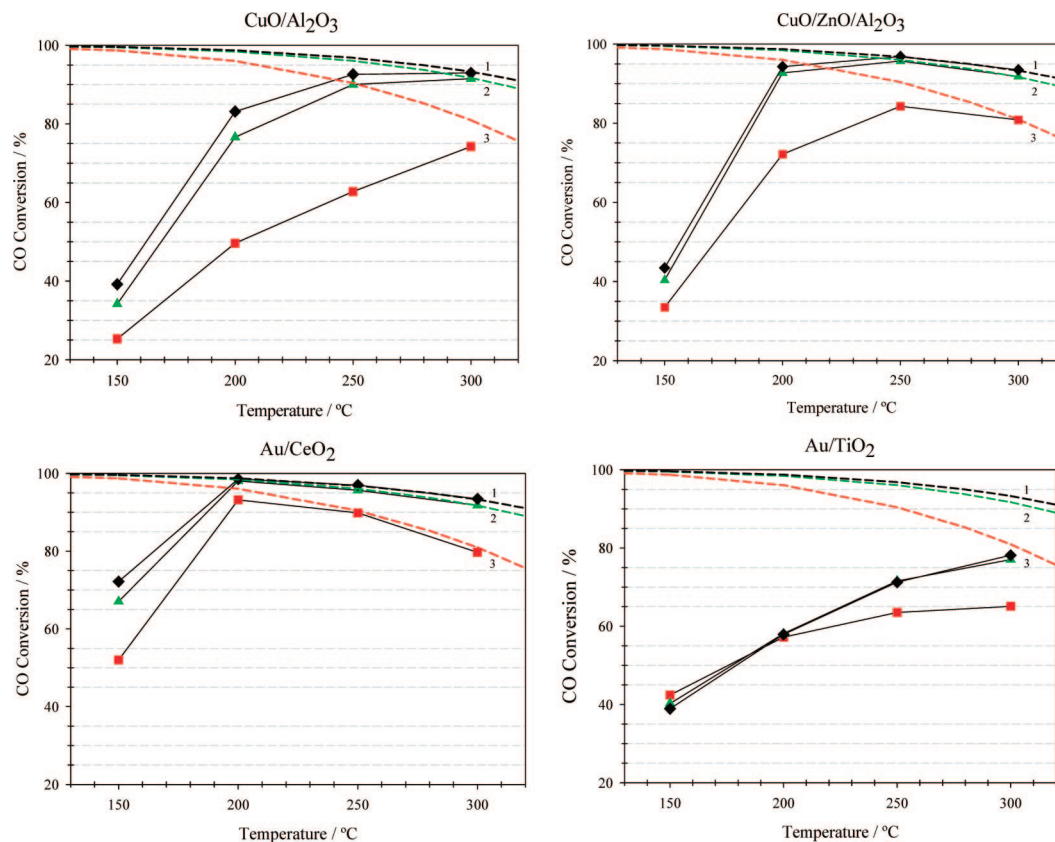


Figure 8. Effect of H₂O content in the feed stream composition over the CO conversion for each catalyst at different temperatures. The lines represent the thermodynamic conversion. Feed composition: (◆, 1) 43.74% H₂O, (▲, 2) 35.39% H₂O, (■, 3) 16.90% H₂O. In all cases the rest of the feed is 4.74% CO, 28.46% H₂, 10.06% CO₂, and the balance N₂.

observed for the Au/CeO₂ catalyst at lower temperatures (section 3.2.4). The decomposition of formates and/or carbonates is favored by the temperature increase, the CO conversion being no longer negatively affected by the CO partial pressure (in most cases it is inclusively positively affected). The temperature range of this transition clearly depends on the performance of each catalytic system. It is therefore important that the usage of empirical power rate laws available in the literature takes into account the temperature range (and other operating conditions) in which the experiments are performed.

The Cu-based catalysts used in this study presented a similar behavior, where the apparent negative order dependence on CO happens in the same temperature range. However, for the Au-based catalysts this does not happen. From Figure 7 it is clear that, for the Au/TiO₂ sample, no positive order dependence on CO was attained in the used range of temperatures. On the other hand, for the Au/CeO₂ sample the positive effect was reached at around 200 °C. Assuming the above-mentioned catalyst's bifunctionality, it is found that the supports responsible for the H₂O activation can be responsible for this difference. As referred to above, the synergistic effects between gold (where CO is adsorbed) and titania are lower than with ceria; therefore, in the latter the formation of intermediate hydroxyl groups (via adsorbed water) is not limiting, so higher CO contents are favorable for a higher activity.

The ceria-supported gold catalyst is, once again, the one that seems to be more promising because it is considerably active and less affected by the CO concentration, at least at low temperatures (150–200 °C). At high temperatures (250–300 °C) CuO/ZnO/Al₂O₃ exhibits a similar performance. Au/TiO₂ is the worst sample, also in agreement with the data of Figure 6.

3.2.3. Effect of the H₂O Content in the Feed. The dependence of the catalysts' performances on the water vapor concentration in the feed stream was also analyzed. It is clearly seen from Figure 8 that, in general, the water vapor content enhances the catalysts' performance in the temperature range 150–300 °C, in agreement with the thermodynamic prediction. This fact is also in agreement with the positive reaction order with respect to water obtained in power law rates.^{23,26–28,42}

For the Au/TiO₂ sample the activity results in the temperature range 150–200 °C are not influenced by the water vapor content. For higher temperatures the increase in the water vapor content above 35.39% (v/v) does not bring any change in the CO conversion, clearly opposed to what happens with the other catalysts. Once again the influence of the support is clearly noticed. The Au/CeO₂ catalyst revealed to be, in terms of catalytic performance, the most promising one since no significant changes were detected with the water vapor concentration, and above 200 °C the conversion reaches the thermodynamic one. It seems therefore that the interaction between gold and ceria, which was highlighted by TPR, results in an activity enhancement. Actually, Rodriguez et al.⁴⁵ pointed out very recently that the noble metal nanoparticles promote the partial reduction of the ceria support by CO or CO/H₂O mixtures, creating in ceria surface oxygen vacancies where the H₂O activation takes place. This evidence corroborates the previous studies by Tabakova et al.,⁴⁶ who have used FTIR spectroscopy to find experimental evidence for modification of ceria in the presence of gold and the appearance of oxygen vacancies at the ceria surface after reduction with hydrogen. The authors stressed the importance of oxygen vacancies and showed that the WGS reaction proceeds at the boundary between small

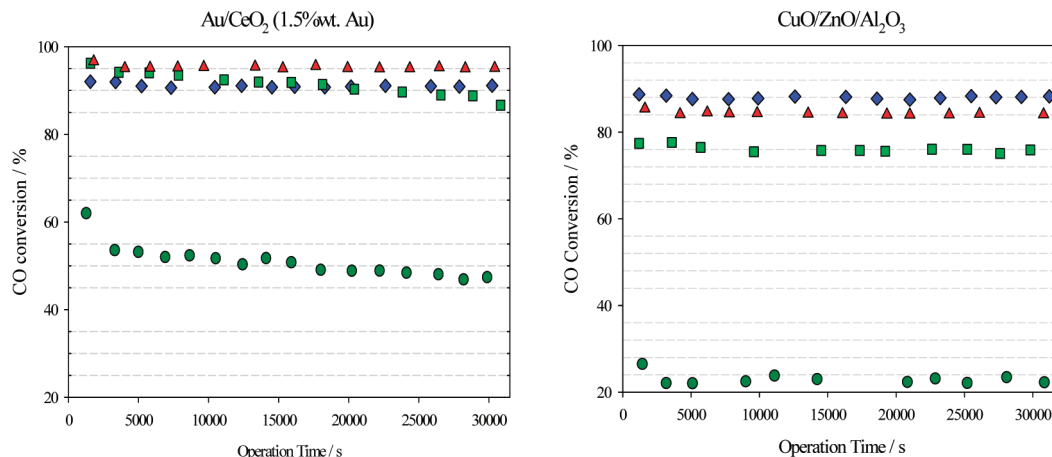


Figure 9. Effect of the time on stream in the WGS activity at different temperatures. Feed composition: 4.74% CO + 35.39% H₂O + 28.46% H₂ + 10.06% CO₂ + 21.35% N₂. Temperature: (◆) 300 °C, (▲) 250 °C, (■) 200 °C, (●) 150 °C.

metallic gold particles and ceria, where CO adsorption on gold and H₂O dissociation on ceria defects take place. The difference in the support reducibility, as well as its capacity to allow the formation of OH groups, might be the responsible for the distinct behavior observed in the WGS activity of the two Au-based catalysts, when the water vapor concentration is changed.

In the literature it is reported that the water content is crucial for the CO conversion performance of a commercial CuO/ZnO catalyst,²² in agreement with our results (Figure 8). Comparing both Cu-based catalysts, it can be seen that the CuO/ZnO/Al₂O₃ catalyst is less influenced by the H₂O concentration. This fact can be connected with the different structures of the Cu particles in each catalyst, described as a possible site for H₂O activation.⁴⁵ However, taking into account the catalyst bifunctionality suggested by Grenoble et al.,³⁶ we may conclude that the support oxide sites are close to the maximum capacity to activate the water vapor. The CuO/ZnO/Al₂O₃ sample exhibits, once again, higher CO conversion than the CuO/Al₂O₃ sample.

3.2.4. Deactivation Tests. An important issue to take into account for the industrial application of any catalyst in hydrogen fuel processing is its stability under WGS conditions. WGS copper-based catalysts are known to be highly stable; however, the gold-based ones, particularly when supported in ceria, have been subjected to extensive work to understand and overcome this problem. Generally, four issues have been widely discussed: (1) the sintering of the metal particles,^{19,47} (2) the “irreversible” over-reduction of the ceria support,⁵ (3) the loss of surface area of ceria,^{11,20} and (4) the blocking of the ceria surface by formation of surface carbonates and/or formates.^{44,48,49}

The two most promising catalysts of this study were then evaluated in terms of their stability. The CO conversion levels were measured at different temperatures after reduction of the samples, and the results are shown in Figure 9. It can be seen that the CuO/ZnO/Al₂O₃ catalyst showed a better stability than Au/CeO₂ under the WGS reaction conditions. CuO/ZnO formulations are known to be deactivated by thermal sintering and/or poisoning of the catalyst surface at temperatures above 300 °C.⁷ In this case, under our experimental conditions, no signs of long-term deactivation were detected, even at 300 °C, which is reported in the literature as being the maximum temperature to avoid the surface migration of the metal particles over the catalyst support. On the other hand, the catalytic activity of Au/CeO₂ decreased progressively at temperatures of 150 and 200 °C, remaining stable at higher temperatures (see Figure 9).

It is therefore clear that the deactivation of such a catalyst is strongly dependent on the temperature. Such deactivation of

Au/CeO₂ seems to be not consistent with literature references about sintering of the gold particles, because when temperature increases, changes in conversion with time are not detectable. It is not possible to establish which deactivation(s) mechanism(s) is/are present (this will be the aim of future work); however, a surface fouling might occur since, at lower temperatures, where the intermediates decomposition is slower, reaction species might block the catalyst sites and consequently decrease the CO conversion. With the temperature increase, the intermediates decomposition is accelerated and no deactivation happens. This idea is in line with the work by Jacobs et al.,⁵⁰ where it was concluded that formates are reaction intermediate species and that at higher temperatures their concentration is limited by the WGS reaction rate, while at lower temperatures the formate surface concentration remains close to the adsorption/desorption equilibrium. Karpenko and coauthors⁴⁴ also justified the deactivation behavior at lower temperatures, now due to the formation of carbonates adsorbed on the ceria support, blocking the sites. Therefore, the carbonate decomposition rate is too low to keep the steady-state carbonate coverage at a low level, promoting the catalyst deactivation. The authors confirmed the carbonate formation, obtaining complete catalyst activity regeneration with an oxidation treatment.

A comparison test in terms of CO conversion obtained for gold/ceria catalysts with different Au loadings (~1.5 and 2.5 wt %) was then performed at 150 °C. The results are presented in Figure 10.

For the catalyst with higher Au loading a higher CO conversion was obtained during the first 30 000 s (~8.3 h). It is reported in the literature that the reaction rate of Au/CeO₂ catalysts varies as a volcano-type curve as a function of the gold metal loading. Maxima at 5 wt %²³ and 3 wt %¹³ were reported. Nevertheless, Figure 10 shows also that the deactivation rate of this catalyst is higher than for the 1.5 wt % Au/ceria catalyst. The activity of the lower Au loading catalyst seems to remain nearly constant, after ca. 20 000 s (~5.6 h), a fact that can be explained by the adsorption/desorption equilibrium of carbonates and/or formates at the catalyst surface. The higher deactivation observed in the 2.5 wt % Au/ceria catalyst might be due to the higher carbonate and/or formate concentration at the catalyst surface, formed at the beginning of the reaction as a consequence of its higher catalytic performance, leading thus to a higher surface coverage and promoting a stronger blocking effect.

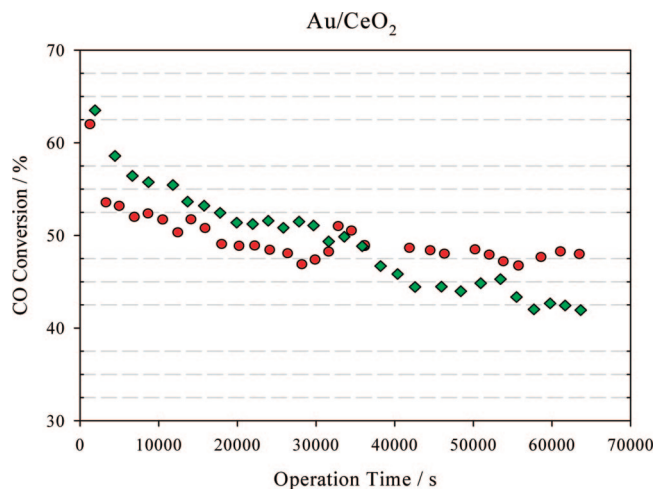


Figure 10. Effect of the operation time on the WGS activity, at 150 °C, for Au/CeO₂ catalysts with different Au loadings. Feed composition: 4.74% CO + 35.39% H₂O + 28.46% H₂ + 10.06% CO₂ + 21.35% N₂. Au loading: (◆) 2.5 wt %, (●) 1.5 wt %.

4. Conclusions

The catalytic performance of Au/TiO₂, Au/CeO₂, CuO/Al₂O₃, and CuO/ZnO/Al₂O₃ catalysts has been investigated for WGS reaction in the low temperature range. It was found that the presence of reaction products in the feed stream has a higher negative effect on CO conversion for Cu-based catalysts when compared with the gold-based ones, namely, at 150 °C. Under the reformat conditions (4.74% CO + 35.39% H₂O + 28.46% H₂ + 10.06% CO₂, balance N₂), the Au/CeO₂ sample is shown to be the most active (particularly at low temperatures, i.e., 150–200 °C). The activity of gold/ceria indicates that the support plays an important role in this reaction catalysis. The commercial CuO/ZnO/Al₂O₃ catalyst showed the best relation of activity/stability. In addition, it was found that the CO concentration present in the reactor feed greatly affects the activity of all catalysts tested. Depending on the reaction temperature, this effect is negative or positive in terms of the catalyst's performance. We also observed that water had a positive effect on CO conversion for all the catalysts, except for the Au/TiO₂ catalyst.

The results of this study indicate that the catalyst selection has to take into account the operation reaction temperature range. At temperatures ≥250 °C Au/CeO₂ is clearly a better option since it seems not to be affected by the deactivation mechanism and shows a higher CO conversion than CuO/ZnO/Al₂O₃. However, at lower temperatures, the stability is a negative factor for its selection and the latter seems to be a better option.

Acknowledgment

Diogo Mendes and Valter Silva are grateful to the Portuguese Foundation for Science and Technology (FCT) for their doctoral grants (SFRH/BD/22463/2005 and SFRH/BD/18159/2004, respectively). We also acknowledge financing from FCT through Projects POCTI/EQU/59345/2004 and PTDC/EQU/ERQ/66045/2006. Finally, we are most grateful to Dr. Oleg Ilinich (BASF) for providing the CuO/Al₂O₃ sample.

Literature Cited

- (1) Energy Information Administration. *International Energy Outlook*; U.S. Department of Energy: Washington, DC, 2007.
- (2) Trimm, D. L.; Onsan, Z. I. Onboard fuel conversion for hydrogen-fuel-cell-driven vehicles. *Catal. Rev.—Sci. Eng.* **2001**, *43* (1–2), 31–84.

- (3) Wee, J. H.; Lee, K. Y. Overview of the development of CO-tolerant anode electrocatalysts for proton-exchange membrane fuel cells. *J. Power Sources* **2006**, *157* (1), 128–135.
- (4) Trimm, D. L. Minimisation of carbon monoxide in a hydrogen stream for fuel cell application. *Appl. Catal., A* **2005**, *296* (1), 1–11.
- (5) Ghenciu, A. F. Review of fuel processing catalysts for hydrogen production in PEM fuel cell systems. *Curr. Opin. Solid State Mater. Sci.* **2002**, *6* (5), 389–399.
- (6) Newsome, D. S. The water-gas shift reaction. *Catal. Rev.—Sci. Eng.* **1980**, *21* (2), 275–318.
- (7) Twigg, M. V.; Spencer, M. S. Deactivation of supported copper metal catalysts for hydrogenation reactions. *Appl. Catal., A* **2001**, *212* (1–2), 161–174.
- (8) Bunluesin, T.; Gorte, R. J.; Graham, G. W. Studies of the water-gas-shift reaction on ceria-supported Pt, Pd, and Rh: Implications for oxygen-storage properties. *Appl. Catal., B* **1998**, *15* (1–2), 107–114.
- (9) Swartz, S. L.; Seabaugh, M. M.; Holt, C. T.; Dawson, W. J. Fuel processing catalysts based on nanoscale ceria. *Fuel Cell Bull.* **2001**, *4* (30), 7–10.
- (10) Cameron, D.; Holliday, R.; Thompson, D. Gold's future role in fuel cell systems. *J. Power Sources* **2003**, *118* (1–2), 298–303.
- (11) Burch, R. Gold catalysts for pure hydrogen production in the water-gas shift reaction: Activity, structure and reaction mechanism. *Phys. Chem. Chem. Phys.* **2006**, *8* (47), 5483–5500.
- (12) Sakurai, H.; Ueda, A.; Kobayashi, T.; Haruta, M. Low-temperature water-gas shift reaction over gold deposited on TiO₂. *Chem. Commun.* **1997**, (3), 271–272.
- (13) Andreeva, D.; Idakiev, V.; Tabakova, T.; Ilieva, L.; Falaras, P.; Bourlinos, A.; Travlos, A. Low-temperature water-gas shift reaction over Au/CeO₂ catalysts. *Catal. Today* **2002**, *72* (1–2), 51–57.
- (14) Andreeva, D.; Idakiev, V.; Tabakova, T.; Andreev, A. Low-temperature water-gas shift reaction over Au/α-Fe₂O₃. *J. Catal.* **1996**, *158* (1), 354–355.
- (15) Tabakova, T.; Idakiev, V.; Andreeva, D.; Mitov, I. Influence of the microscopic properties of the support on the catalytic activity of Au/ZnO, Au/ZrO₂, Au/Fe₂O₃, Au/Fe₂O₃-ZnO, Au/Fe₂O₃-ZrO₂ catalysts for the WGS reaction. *Appl. Catal., A* **2000**, *202* (1), 91–97.
- (16) Idakiev, V.; Tabakova, T.; Naydenov, A.; Yuan, Z. Y.; Su, B. L. Gold catalysts supported on mesoporous zirconia for low-temperature water-gas shift reaction. *Appl. Catal., B* **2006**, *63* (3–4), 178–186.
- (17) Fu, Q.; Saltsburg, H.; Flytzani-Stephanopoulos, M. Active non-metallic Au and Pt species on ceria-based water-gas shift catalysts. *Science* **2003**, *301* (5635), 935–938.
- (18) Yuan, Z. Y.; Idakiev, V.; Vantomme, A.; Tabakova, T.; Ren, T. Z.; Su, B. L. Mesoporous and nanostructured CeO₂ as supports of nano-sized gold catalysts for low-temperature water-gas shift reaction. *Catal. Today* **2008**, *131* (1–4), 203–210.
- (19) Luengnarumitchai, A.; Osuwan, S.; Gulari, E. Comparative studies of low-temperature water-gas shift reaction over Pt/CeO₂, Au/CeO₂, and Au/Fe₂O₃ catalysts. *Catal. Commun.* **2003**, *4* (5), 215–221.
- (20) Fu, Q.; Deng, W. L.; Saltsburg, H.; Flytzani-Stephanopoulos, M. Activity and stability of low-content gold-cerium oxide catalysts for the water-gas shift reaction. *Appl. Catal., B* **2005**, *56* (1–2), 57–68.
- (21) Chane-Ching, J. Y. New cerium (IV) cpd.—Easily dispersible in water to form stable sols. EP208580, 1987.
- (22) Ginés, M. J. L.; Amadeo, N.; Laborde, M.; Apesteguia, C. R. Activity and structure-sensitivity of the water-gas shift reaction over Cu-Zn-Al mixed-oxide catalysts. *Appl. Catal., A* **1995**, *131* (2), 283–296.
- (23) Leppelt, R.; Schumacher, B.; Plzak, V.; Kinne, M.; Behm, R. J. Kinetics and mechanism of the low-temperature water-gas shift reaction on Au/CeO₂ catalysts in an idealized reaction atmosphere. *J. Catal.* **2006**, *244* (2), 137–152.
- (24) Bocuzzi, F.; Chiorino, A.; Manzoli, M.; Lu, P.; Akita, T.; Ichikawa, S.; Haruta, M. Au/TiO₂ nanosized samples: A catalytic, TEM, and FTIR study of the effect of calcination temperature on the CO oxidation. *J. Catal.* **2001**, *202* (2), 256–267.
- (25) Moe, J. M. Design of water-gas shift reactors. *Chem. Eng. Prog.* **1962**, *58* (3), 33–36.
- (26) Ayastuy, J. L.; Gutierrez-Ortiz, M. A.; Gonzalez-Marcos, J. A.; Aranzabal, A.; Gonzalez-Velasco, J. R. Kinetics of the low-temperature WGS reaction over a CuO/ZnO/Al₂O₃ catalyst. *Ind. Eng. Chem. Res.* **2005**, *44* (1), 41–50.
- (27) Amadeo, N. E.; Laborde, M. A. Hydrogen-production from the low-temperature water-gas shift reaction—Kinetics and simulation of the industrial reactor. *Int. J. Hydrogen Energy* **1995**, *20* (12), 949–956.
- (28) Ovesen, C. V.; Stoltze, P.; Norskov, J. K.; Campbell, C. T. A kinetic-model of the water gas shift reaction. *J. Catal.* **1992**, *134* (2), 445–468.

- (29) Yurieva, T. M.; Plyasova, L. M.; Kriger, T. A.; Zaikovskii, V. I.; Makarova, O. V.; Minyukova, T. P. State of copper-containing catalyst for methanol synthesis in the reaction medium. *React. Kinet. Catal. Lett.* **1993**, *51* (2), 495–500.
- (30) Fujitani, T.; Saito, M.; Kanai, Y.; Kakumoto, T.; Watanabe, T.; Nakamura, J.; Uchijima, T. The role of metal-oxides in promoting a copper catalyst for methanol synthesis. *Catal. Lett.* **1994**, *25* (3–4), 271–276.
- (31) Koryabkina, N. A.; Phatak, A. A.; Ruettinger, W. F.; Farrauto, R. J.; Ribeiro, F. H. Determination of kinetic parameters for the water-gas shift reaction on copper catalysts under realistic conditions for fuel cell applications. *J. Catal.* **2003**, *217* (1), 233–239.
- (32) Campbell, C. T.; Daube, K. A. A surface science investigation of the water-gas shift reaction on Cu(111). *J. Catal.* **1987**, *104* (1), 109–119.
- (33) Shido, T.; Iwasawa, Y. Reactant-promoted reaction-mechanism for water-gas shift reaction on ZnO, as the genesis of surface catalysis. *J. Catal.* **1991**, *129* (2), 343–355.
- (34) Ghiotti, G.; Boccuzzi, F. Chemical and physical-properties of copper-based catalysts for CO shift reaction and methanol synthesis. *Catal. Rev.—Sci. Eng.* **1987**, *29* (2–3), 151–182.
- (35) Shishido, T.; Yamamoto, M.; Atake, I.; Li, D. L.; Tian, Y.; Morioka, H.; Honda, M.; Sano, T.; Takehira, K. Cu/Zn-based catalysts improved by adding magnesium for water-gas shift reaction. *J. Mol. Catal. A* **2006**, *253* (1–2), 270–278.
- (36) Grenoble, D. C.; Estadt, M. M.; Ollis, D. F. The chemistry and catalysis of the water gas shift reaction 0.1. The kinetics over supported metal-catalysts. *J. Catal.* **1981**, *67* (1), 90–102.
- (37) Jacobs, G.; Graham, U. M.; Chenu, E.; Patterson, P. M.; Dozier, A.; Davis, B. H. Low-temperature water-gas shift: Impact of Pt promoter loading on the partial reduction of ceria and consequences for catalyst design. *J. Catal.* **2005**, *229* (2), 499–512.
- (38) Panagiotopoulou, P.; Christodoulakis, A.; Kondarides, D. I.; Boghosian, S. Particle size effects on the reducibility of titanium dioxide and its relation to the water-gas shift activity of Pt/TiO₂ catalysts. *J. Catal.* **2006**, *240* (2), 114–125.
- (39) Frost, J. C. Junction effect interactions in methanol synthesis catalysts. *Nature* **1988**, *334* (6183), 577–580.
- (40) Golunski, S.; Rajaram, R.; Hodge, N.; Hutchings, G. J.; Kiely, C. J. Low-temperature redox activity in co-precipitated catalysts: A comparison between gold and platinum-group metals. *Catal. Today* **2002**, *72* (1–2), 107–113.
- (41) Idakiev, V.; Tabakova, T.; Yuan, Z. Y.; Su, B. L. Gold catalysts supported on mesoporous titania for low-temperature water-gas shift reaction. *Appl. Catal., A* **2004**, *270* (1–2), 135–141.
- (42) Salmi, T.; Hakkarainen, R. Kinetic-study of the low-temperature water-gas shift reaction over a Cu-ZnO catalyst. *Appl. Catal.* **1989**, *49* (2), 285–306.
- (43) Rhodes, C.; Hutchings, G. J.; Ward, A. M. Water-gas shift reaction—Finding the mechanistic boundary. *Catal. Today* **1995**, *23* (1), 43–58.
- (44) Karpenko, A.; Leppelt, R.; Cai, J.; Plzak, V.; Chuvilin, A.; Kaiser, U.; Behm, R. J. Deactivation of a Au/CeO₂ catalyst during the low-temperature water-gas shift reaction and its reactivation: A combined TEM, XRD, XPS, DRIFTS, and activity study. *J. Catal.* **2007**, *250* (1), 139–150.
- (45) Rodriguez, J. A.; Liu, P.; Hrbek, J.; Evans, J.; Perez, M. Water gas shift reaction on Cu and Au nanoparticles supported on CeO₂(111) and ZnO(0001)over-bar: Intrinsic activity and importance of support interactions. *Angew. Chem., Int. Ed.* **2007**, *46* (8), 1329–1332.
- (46) Tabakova, T.; Boccuzzi, F. B.; Manzoli, M.; Andreeva, D. FTIR study of low-temperature water-gas shift reaction on gold/ceria catalyst. *Appl. Catal., A* **2003**, *252* (2), 385–397.
- (47) Wang, X.; Gorte, R. J.; Wagner, J. P. Deactivation mechanisms for Pd/ceria during the water-gas-shift reaction. *J. Catal.* **2002**, *212* (2), 225–230.
- (48) Deng, W. L.; Flytzani-Stephanopoulos, M. On the issue of the deactivation of Au-ceria and Pt-ceria water-gas shift catalysts in practical fuel-cell applications. *Angew. Chem., Int. Ed.* **2006**, *45* (14), 2285–2289.
- (49) Kim, C. H.; Thompson, L. T. Deactivation of Au/CeO_x water gas shift catalysts. *J. Catal.* **2005**, *230* (1), 66–74.
- (50) Jacobs, G.; Williams, L.; Graham, U.; Thomas, G. A.; Sparks, D. E.; Davis, B. H. Low temperature water-gas shift: In situ DRIFTS-reaction study of ceria surface area on the evolution of formates on Pt/CeO₂ fuel processing catalysts for fuel cell applications. *Appl. Catal., A* **2003**, *252* (1), 107–118.

Received for review July 11, 2008

Revised manuscript received October 1, 2008

Accepted October 16, 2008

IE8010676